Inorg. Chem. **2005**, *44*, 1381–1390

Atomic Silicon in Siloxanic Networks: The Nature of the Oxo-Oxygen–Silicon Bond

P. Belanzoni,*,† G. Giorgi,‡ G. F. Cerofolini,§ and A. Sgamellotti‡

CNR-ISTM and Dipartimento di Chimica, Università di Perugia, Via Elce di Sotto 8, 06123, Perugia PG, Italy, and STMicroelectronics, Stradale Primosole 50, 95100 Catania CT, Italy

Received August 5, 2004

The existence of atomic silicon cryptates in siloxanic networks has been studied theoretically via density functional calculations. By modeling with model molecules the candidate sites to host atomic silicon, we found that metastable adducts can be formed only in regions where the siloxanic network is not subjected to steric constraints; stationary states are instead unstable in highly reticulated siloxanic networks. The nature of the oxo-oxygen–silicon bond at the SiO_2 surface is analyzed in detail. It is concluded that silicon is kept at the surface in atomic-like configuration by (i) σ charge donation from oxo-oxygen atoms into the empty silicon p_σ orbital; (ii) π charge back-donation from singly occupied silicon $3p_\pi$ orbitals into empty σ^* model molecule orbitals. Surprisingly, these results attribute to atomic silicon the character of bifunctional Lewis acid.

1. Introduction

Though our knowledge of the structure of matter was initiated by atomic spectroscopy, only a few atomic systems (with the obvious exception of noble gases) have been studied in detail. The hybridization energy of most atoms is indeed so low that they can easily react to form clusters. This is especially true in a condensed phase where matter transport does not limit the process. In the past few years, however, methods for the preparation and stabilization of nearly free atomic species have been developed. Among them, the most common one is the low-rate incorporation of atoms from the gas phase in a film of an inert species (like noble gases) condensing at a fast rate on a cool substrate. In this way, as long as the substrate temperature and density of trapped atoms are kept low, nearly free atomic species can be studied.

Atomic silicon in such conditions has in recent years been the matter of some spectroscopic studies, not only in noble gases but also in other chemically robust species.[1] It has recently been proposed by Kageshima, Shiraishi, and Uematsu (KSU) that atomic silicon is also generated at the $Si-SiO_2$ interface during the high-temperature oxidation in dry O_2.[2,3] That such a state may survive in the severe oxidation conditions may seem difficult, and indeed, KSU proposed that it migrates to the surface where out-diffuses as volatile SiO or transforms to SiO_2. However, the anomalous reactivities (compared to that of the oxide underneath) toward O_2[4] and H_2[5] manifested by the SiO_2 surface might perhaps be explained in terms of distribution of atomic silicon (or cluster of a few atoms) embedded in the siloxanic network forming a kind of atomic cryptate. This hypothesis is supported by the high stability of the siloxo structure and by the fact that, though the redox reaction, in which atomic silicon cleaves two siloxanic bridges

$$\mathrm{Si}^{(0)} + 2(-\mathrm{O})_3\mathrm{Si}^{(4)}\mathrm{OSi}^{(4)}(\mathrm{O}-)_3 \downarrow [(-\mathrm{O})_3\,\mathrm{Si}^{(3)}]_2\mathrm{Si}^{(2)}[\mathrm{OSi}^{(4)}(\mathrm{O}-)_3]_2 \quad (1)$$

is in the absence of strong steric constraints a highly exothermic process [by ca. $2E_b(\mathrm{Si}-\mathrm{Si}) \simeq 6$ eV, where $E_b(\mathrm{Si}-\mathrm{Si})$ is the Si−Si bond energy], the activation energy

* To whom correspondence should be addressed. E-mail: paola@thch.unipg.it. Fax: +39-075-5855606.
† Dipartimento di Chimica, Università di Perugia.
‡ CNR-ISTM and Dipartimento di Chimica, Università di Perugia.
§ STMicroelectronics.

(1) Maier, G.; Reisenauer, H. P.; Egenolf, H.; Glatthaar, J. *Silicon Chemistry—From the Atom to Extended Systems*; Jutzi, P., Schubert, U., Eds.; Wiley-VCH: New York, 2003; p 4.
(2) Kageshima, H.; Shiraishi, K. *Phys. Rev. Lett.* **1998**, *81*, 5936.
(3) Kageshima, H.; Shiraishi, K.; Uematsu, M. *Jpn. J. Appl. Phys.* **1999**, *38*, L971.
(4) Gusev, E. P.; Lu, H. C.; Gustafsson, T.; Garfunkel, E. *Phys. Rev. B* **1995**, *52*, 1759.
(5) Baumvol, I. J. R.; Gusev, E. P.; Stedile, F. C.; Freire, F. L., Jr.; Green, M. L.; Brasen, D. *Appl. Phys. Lett.* **1998**, *72*, 450.

10.1021/ic048927d CCC: $30.25
Published on Web 01/29/2005

required to cleave the Si−O bridge forming the silica network is high. That reaction 1 may indeed require a high activation energy is strongly supported by the fact that interfacial reaction

$$Si(s) + SiO_2(s) \rightarrow 2SiO(g)$$

in the absence of oxygen does really occur, but only at temperatures higher than 1000 °C.

Atomic silicon can achieve an octet configuration by donation of lone pairs from two oxygen atoms of two oxo bridges between silicon, the resulting Lewis formula of the center being

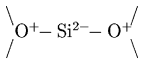

0

where an unterminated bond implies bonding to silicon (or to hydrogen, at the surface of hydroxylated silica).

To test the hypothesis that atomic silicon survives in SiO_2 and, in that case, which is the nature of the bonding with the oxo-oxygen at the surface, we have performed density functional calculations, using model molecules to mimic the oxide.

Of course, the theoretical possibility of such states does not guarantee that they are actually found in the considered oxidation conditions, even assuming that the putatively high activation energy required for reaction 1 prevents it from occurring, atomic silicon is expected to wander through the oxide until meets another silicon atom and forms a cluster. Actually, the experimental evidence of the presence of silicon dimers at the surface reported in ref 6 requires necessarily the existence of long living monomer species as precursors of these dimers; that anyway makes it useful as a study of the oxide region where silicon atoms are most stable.

2. Methods

2.1. Choice of the Model Molecules. The thin (in the nanometer length scale) oxide grown via thermal oxidation in O_2 of hydrogen-terminated silicon is highly heterogeneous because of the existence of several regions with different compositions: an interfacial region, with thickness of a few angstroms in which the stoichiometry changes swiftly from Si to SiO_2 (through all intermediate oxidation states $Si^{(n)}$, $n = 1, 2, 3$); a bulk region, whose stoichiometry is very close to that of SiO_2; and a superficial region expectedly containing a lot of silanol terminations. The substitution of silanol terminations for disiloxo bridges produces a progressive loss of reticulation on going from the bulk region to the surface one. The combination of this complicated environment with the amorphous nature of SiO_2 makes it manifestly difficult to mimic the oxide either with a single molecule or with a two-dimensional lattice. We therefore try to model the situation with different molecules in the various zones.

(i) The interfacial region is ignored because it is the source of the stress eventually producing atomic silicon and is thus presumed not to be able to host a foreign atom. (ii) For the superficial region we consider two extreme situations, one characterized by extremely weak steric constraints (as for surfaces whose siloxanic network was almost completely destroyed by the cleavage of the oxo bridges by water molecules) and the other characterized by extremely strong steric constraints (as for hydrophobic surfaces with only few hydroxyl terminations).

Table 1. Molecules Used To Mimic Silicon Hosting Sites at the SiO_2 Surface

molecule	referred to as
$H_3SiOSiH_3$ (in pair)	**1**
$H_3SiOSiH_2OH$ (in pair)	**2**
$(HO)_3SiOSi(OH)_3$ (in pair)	**3**
$H_3SiO(SiH_2O)_2SiH_3$	**4**
$H_3SiO(SiH_2O)_4SiH_3$	**5**
$HOSi(H_2)O(SiH_2O)_4Si(H_2)OH$	**6**
$H_3SiO(SiH_2O)_6SiH_3$	**7**

The weak steric constraints in the superficial region are modeled describing a candidate superficial hosting site either with a pair of uncorrelated molecules or with linear molecules with *n* oxo bridges. Table 1 lists the molecules considered in this work, while Figure 1 shows their stick-and-ball prospect view, each of them in a conformation of local energy minimum in which oxygen atoms in position 1 and *n* are facing one another. Molecules **1**, **2**, and **3** are used to study how the binding energy of adduct 0 depends on the assumed nearest neighbor distribution. Molecules **4**, **5**, **6**, **7** and a pair of **1** are used to study the effect of strain (decreasing in the order $\mathbf{2}_2 \lesssim \mathbf{1}_2 \ll \mathbf{7} \lesssim \mathbf{6} < \mathbf{5} \ll \mathbf{4}$ for silicon between terminal oxo-oxygens). The effect of strain is also evaluated considering, for each molecule **5** and **7**, the adducts obtained putting the atomic silicon between oxo-oxygen 1 and *n*, 2 and $n - 1$, 3 and $n - 2$, and so on. Referring to these configurations as

$$|\overset{1}{O}\rangle Si\langle\overset{n}{O}|,|\overset{2}{O}\rangle Si\langle\overset{n-1}{O}|,|\overset{3}{O}\rangle Si\langle\overset{n-2}{O}|,...$$

they are ordered for increasing stress and may be reasonably assumed to represent the strain condition on going from the surface to the bulk of SiO_2. Unreconstructable hydrophobic surfaces as well as the bulk region of the oxide are instead modeled considering the silicon atom either at the outer surfaces or within the cages of polysilsesquioxanes **8** and **9** in Figure 1.

2.2. Computational and Methodological Details. The molecules were modeled using the Amsterdam Density Functional (ADF) program package.[7−10] In the ADF code, the one-electron Kohn−Sham equations are solved self-consistently using highly efficient numerical techniques,[11] and a density fitting procedure is employed to obtain accurate Coulomb and exchange potentials in each self-consistent-field cycle. In the calculations, the molecular orbitals were expanded in a basis set of Slater type orbitals (STOs), and the frozen core approximation was used for the evaluation of valence orbitals. The parametrization of electron gas data[12] by Vosko, Wilk, and Nusair[13] was employed in the local density approximation. Full geometry optimizations were performed within spin unrestricted (triplet) approach including Becke's gradient corrections[14] to the exchange part of the potential and Perdew's

(6) Zandvliet, H. J. W.; Poelsema, B.; Swartzentruber, B. S. *Phys. Today* **2001** *54*, 40.

(7) Baerends, E. J.; Ellis, D. E.; Ros, P. *Chem. Phys.* **1973**, *2*, 42.
(8) *ADF2002.01*; SCM, Theoretical Chemistry, Vrije Universiteit: Amsterdam, The Netherlands, http://www.scm.com.
(9) te Velde, G.; Bickelhaupt, F. M.; van Gisbergen, S. J. A.; Fonseca Guerra, C.; Baerends, E. J.; Snijders, J. G.; Ziegler, T. *J. Comput. Chem.* **2001**, *22*, 931.
(10) Fonseca Guerra, C.; Snijders, J. G.; te Velde, G.; Baerends, E. J. *Theor. Chem. Acc.* **1998**, *99*, 391.
(11) te Velde, G.; Baerends, E. J. *J. Comput. Phys.* **1992**, *99*, 84.
(12) Ceperley D. M.; Alder, B. J. *Phys. Rev. Lett.* **1980**, *45*, 566.
(13) Vosko, S. H.; Wilk, L.; Nusair, M. *Can. J. Phys.* **1980**, *58*, 1200.
(14) Becke, A. D. *Phys. Rev. A* **1988**, *38*, 3098.

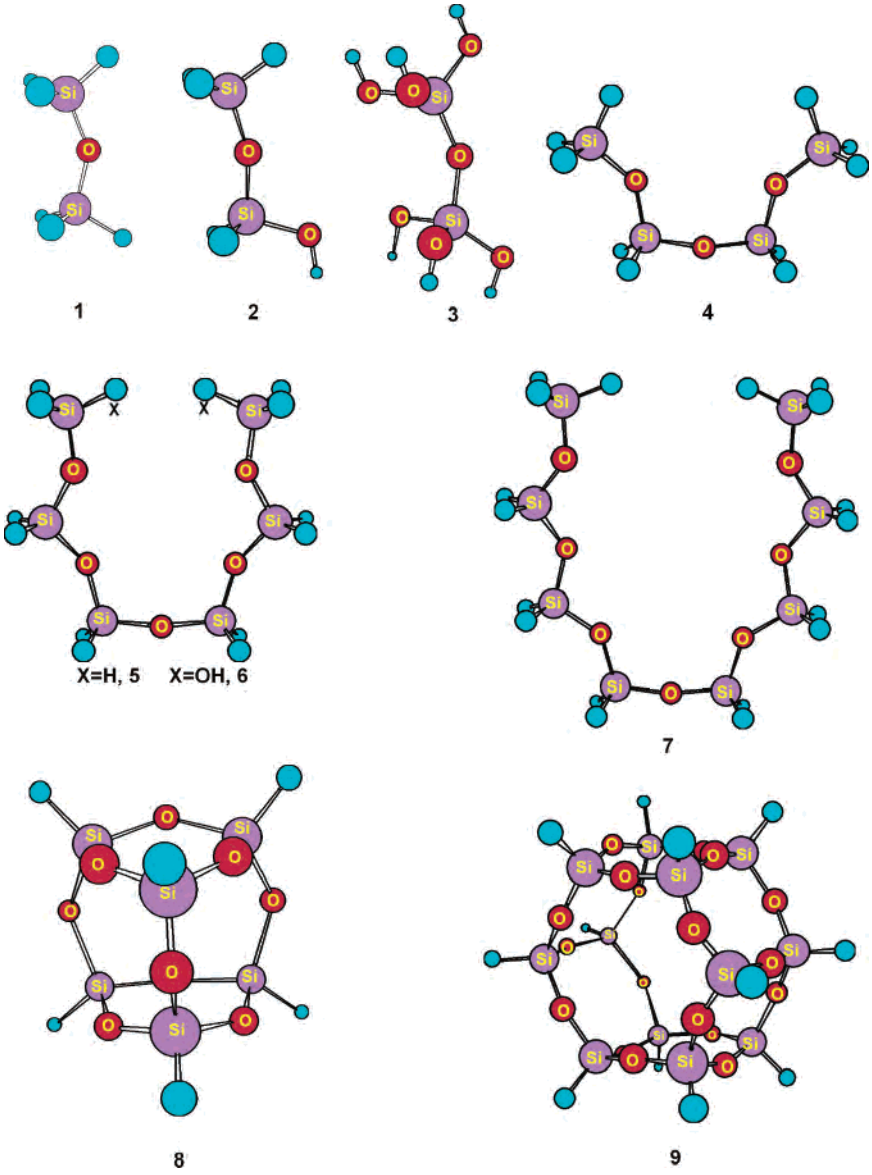

Figure 1. The molecules considered for the formation of adducts with atomic silicon.

gradient correction[15,16] to the correlation. For the model molecules, the Si, O, and H molecular orbitals were expanded in a triple-ζ STO basis set, adding as polarization functions one 2p and one 3d STO for H and O, respectively, and one 3d plus one 4f STO for Si. The core orbitals (from 1s to 2p for Si, and 1s for O) were kept frozen. The basis set superposition error (BSSE) has been calculated for the adduct $\mathbf{1}_2'$ to be 0.007 eV (1% of the bonding energy with respect to reactants). The chosen basis set size appears to be satisfactory.

To analyze the oxo-oxygen−silicon interaction energies, we used a method that is an extension of the well-known decomposition scheme of Morokuma.[17] The bonding energy is decomposed into a number of terms. The first term, $\Delta E°$, is obtained from the energy of the wave function ψ^0 which is constructed as the antisymmetrized and renormalized product of the wave functions ψ^A and ψ^B of the fragments A and B from which the molecule is built up. $\Delta E°$, which is called steric repulsion, consists of two components. The first is the electrostatic interaction, ΔE_{elstat}, of the nuclear charges and unmodified electronic charge density of one fragment with those of the other fragment, both fragments being at their final positions. The second component is the so-called exchange repulsion or Pauli repulsion, ΔE_{Pauli}, which is essentially due to the antisymmetry requirement of the total wave function. In addition to the steric repulsion term $\Delta E°$, there are the attractive orbital interactions which enter when the wave function ψ^0 is allowed to relax to the fully converged ground-state wave function of the total molecule, ψ^{AB}. The energy lowering due to mixing of virtual orbitals of the fragments into the occupied orbitals is called orbital interaction energy, ΔE_{oi}, that includes both the charge transfer and polarization interactions. This term, according to the decomposition scheme proposed by Ziegler,[18] may be broken up into contributions from the orbital interactions within the various irreducible representations of the overall symmetry group of the system. There is a third contribution to the total bonding energy ($\Delta E = \Delta E° + \Delta E_{oi}$) in the frequent cases where the ground-state wave functions ψ^A and ψ^B, at the equilibrium geometries of the free fragments, cannot be

(15) Perdew, J. P. *Phys. Rev. B* **1986**, *33*, 8822.
(16) Perdew, J. P. *Phys. Rev. B* **1986**, *34*, 7406.
(17) (a) Morokuma, K. *J. Chem. Phys.* **1971**, *55*, 1236. (b) Kitaura, K.; Morokuma, K. *Int. J. Quantum Chem.* **1976**, *10*, 325.
(18) Ziegler, T.; Rauk, A. *Theor. Chim. Acta* **1977**, *46*, 1.

used to calculate $\Delta E°$. The geometry of the free fragment is often different from the geometry of the fragments as it occurs in the overall molecule. Also, the ground electronic configuration of the free fragment may not be suitable for interaction with the other fragment. The energy required to prepare the fragments for interaction by changing the geometry and the electronic configuration is called preparation energy, ΔE_{prep}. Thus the total bonding energy will be

$$\Delta E = \Delta E_{prep} + \Delta E° + \Delta E_{oi}$$

3. Results

3.1. Geometrical Structure. Figures 2−5 show the most stable adducts resulting from the reaction of atomic silicon with the molecules shown in Figure 1. The optimized geometrical parameters are also shown, with internuclear distances in angstroms and angles in degrees. The symbols have the following meaning:

$$2\mathbf{N} + \mathrm{Si} \rightarrow \mathbf{N}_2' \text{ for } \mathbf{N} = 1, 3$$

$$2\mathbf{2} + \mathrm{Si} \rightarrow \mathbf{2}_2^{(0)} \text{ for } |\mathrm{HO}\rangle\, \mathrm{Si}\, \langle \mathrm{OH}|$$

$$\mathbf{N} + \mathrm{Si} \rightarrow \mathbf{N}' \text{ for } \mathbf{N} > 3 \text{ and } |\overset{1}{\mathrm{O}}\rangle\, \mathrm{Si}\, \langle \overset{n}{\mathrm{O}}|$$

$$\mathbf{N} + \mathrm{Si} \rightarrow \mathbf{N}'' \text{ for } \mathbf{N} > 3 \text{ and } |\overset{2}{\mathrm{O}}\rangle\, \mathrm{Si}\, \langle \overset{n-1}{\mathrm{O}}|$$

$$\mathbf{N} + \mathrm{Si} \rightarrow \mathbf{N}''' \text{ for } \mathbf{N} > 3 \text{ and } |\overset{3}{\mathrm{O}}\rangle\, \mathrm{Si}\, \langle \overset{n-2}{\mathrm{O}}|$$

The Si−O distance ranges from 2.39 to 2.48 Å for $\mathbf{N} = 1$, 2, 3, and spans a larger field from 2.21 to 2.61 Å for $\mathbf{N} > 3$, with a value of 2.18 Å for $\mathbf{N} = 8$ and 2.23 Å for $\mathbf{N} = 9$.

More interestingly, these structures show that the Si−O−Si angle of the disiloxo center involved in the interaction with Si changes from ca. 180° in **4**, **5**, and **7** (before the reaction) to 126° in **4′**, 128° in **5″**, and 125° in **7‴** (after the reaction), and from ca. 144° to 132° in **5′**, 129° in **7′**, and 124° in **7″**. In $\mathbf{6}^{(0)}$ and $\mathbf{2}_2^{(0)}$, the terminal H−O−Si angle involved in the bonding with Si does not change after the reaction, remaining ca. 118°, with the Si bonding to O with an angle of 143° and 134°, respectively. Finally, in $\mathbf{1}_2'$ and $\mathbf{3}_2'$ the Si−O−Si angle of the disiloxo center is close to the value before the reaction, i.e., ca. 140°.

After reaction with Si, the oxygen bond configuration becomes thus very similar to that resulting after protonation; i.e., a trivalent, 3-fold coordinated oxygen can be found in all the adducts.

3.2. Energetics. As a general result, the triplet state of the adducts is always the configuration of minimum energy. Table 2 gives the total energy of the adducts shown in Figures 2−5 with respect to atoms (E) together with the reaction enthalpies (ΔE) of the adducts with respect to reactants. A negative ΔE means that the adduct is more stable than reactants. In all cases, the adducts are found to be thermodynamically more stable than reactants. The binding energy, however, increases when the reacting molecules are sufficiently flexible to adapt the configuration of the oxo centers to atomic silicon; otherwise, one oxo-oxygen atom may react with atomic silicon, and the adduct can be less stable than reactants. In general, however, the addition of a silicon atom to an open siloxanic network stabilizes it.

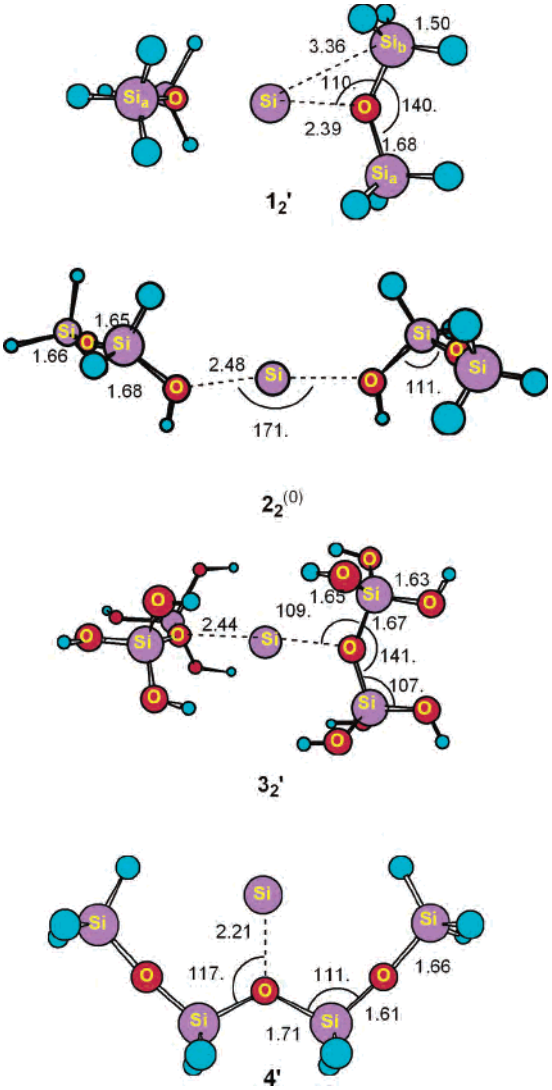

Figure 2. The $\mathbf{1}_2'$, $\mathbf{2}_2^{(0)}$, $\mathbf{3}_2'$, and **4′** adducts resulting from the reaction of atomic silicon with molecules shown in Figure 1.

The comparison of the binding energies of $\mathbf{1}_2'$ and $\mathbf{3}_2'$ shows that the energy stabilizing the adducts is substantially independent of silicon terminations. All molecules not imposing strong steric constraints to the formation of center **0** (i.e., pairs of **1**, **2**, and **3**) were actually found to be able to form with silicon a stable adduct with respect to reactants with the binding energy decreasing steadily along the chain from a value which is higher the longer the molecule. Of course, the stabilizing energy decreases with the steric constraint hindering the formation of the adduct. That the strain controls the binding energy is confirmed by the steady decrease of $|\Delta E|$ from −11.1 kcal/mol in $\mathbf{6}^{(0)}$ to −3.0 kcal/mol in **5″** through −6.5 kcal/mol in **5′**. A similar conclusion is obtained comparing equivalent positions in molecules of different length (and hence flexibility): −6.5 kcal/mol in **5′** versus −7.8 kcal/mol in **7′**.

The search of bound states of $\mathrm{Si}^{(0)} + \mathbf{8}$ and $\mathrm{Si}^{(0)} + \mathbf{9}$ started assuming as initial guesses either the center of the siloxanic

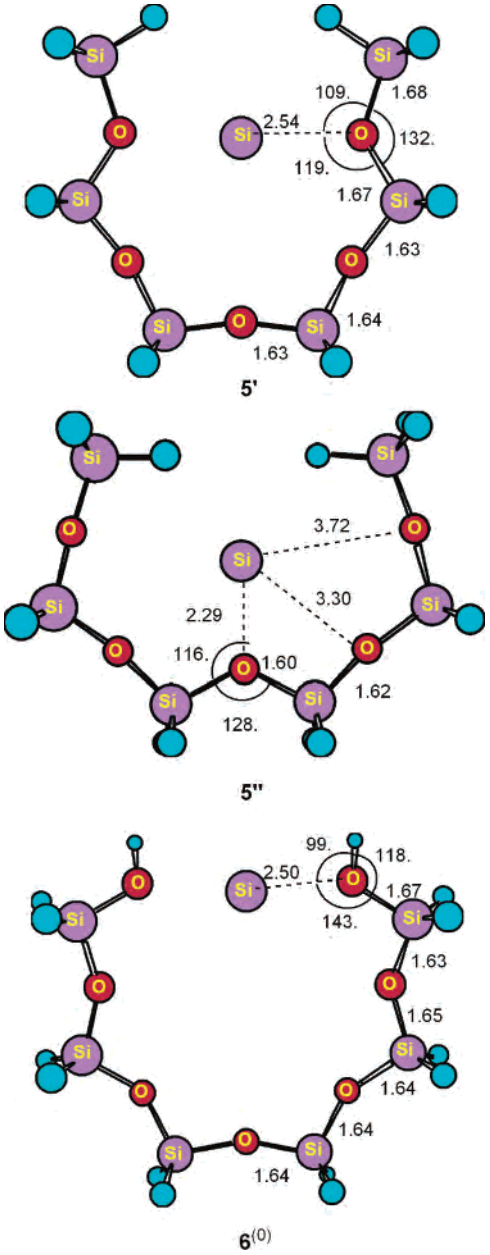

Figure 3. The 5′, 5″, and $\mathbf{6}^{(0)}$ adducts resulting from the reaction of atomic silicon with molecules shown in Figure 1.

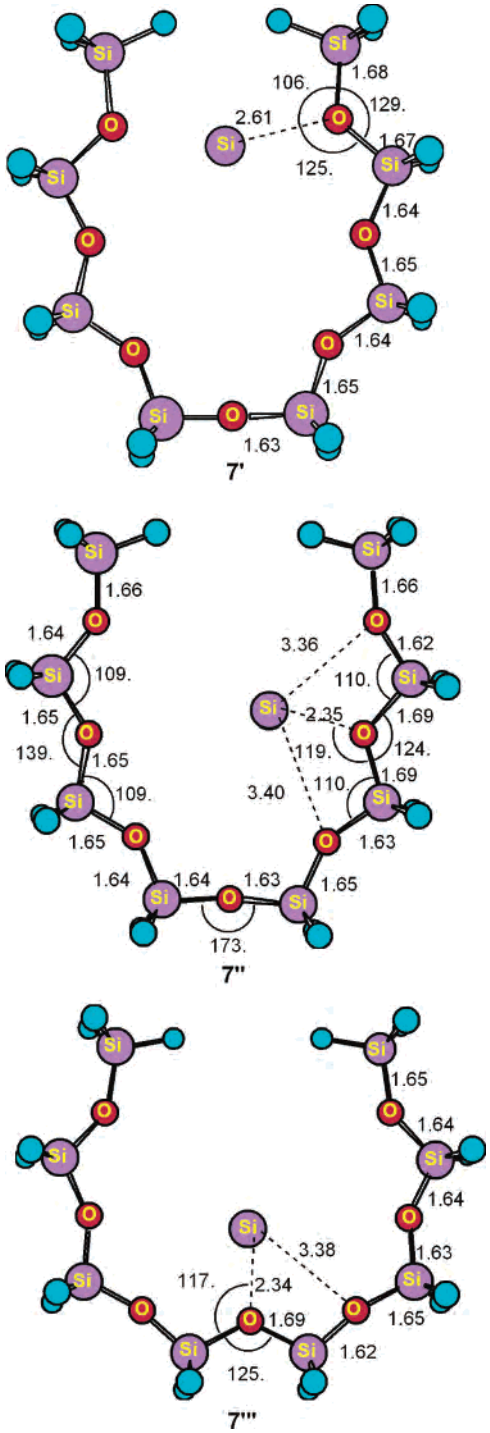

Figure 4. The 7′, 7″, and 7‴ adducts resulting from the reaction of atomic silicon with molecules shown in Figure 1.

cage or the middle point on the segment joining two oxygen atoms linking the upper and lower faces of the cages. In both cases, no stationary states with $Si^{(0)}$ inside the cage were found. Rather, stationary states were found with $Si^{(0)}$ outside the cages on the top of one siloxanic oxygen; the energy of these complexes is lower than that of the reactants by 8.5 kcal/mol for **8′** and 6.7 kcal/mol for **9′**.

3.3. Discussion. 3.3.1. The Nature of the Oxo-Oxygen−Silicon Bond. Electronic Structure. Table 3 shows selected one-electron α spin-orbitals obtained by spin unrestricted calculations for the adduct series. The energies and the percentage composition based on Mulliken population analysis are given in terms of silicon atom and **N** orbitals. Only the molecular orbitals showing remarkable interactions between Si atom and **N** have been reported. Moreover, for adducts $\mathbf{2}_2^{(0)}$−**8′**, only σ (α spin) molecular orbitals showing the largest silicon $3p_\sigma$ percentage have been reported. Focusing on $\mathbf{1}_2'$ as prototype adduct for evaluating the nature of the oxo-oxygen−silicon bond, we see that the most important molecular orbitals of the model molecule **1** interacting with silicon atom orbitals are the occupied $3a_1$ and $4a_1$ and the unoccupied $5b_1$ orbitals. They are depicted in Figure 6 which shows the orbital interaction diagram between Si atom and a pair of **1**. The $\mathbf{1}_2'$ adduct is chosen to lie with the O−Si−O framework along the *z* axis, with the **1** denoted (1) in the *xz* plane, and with the **1** denoted (2) in the *yz* plane. The $3a_1$ orbital of **1** can be described as oxygen

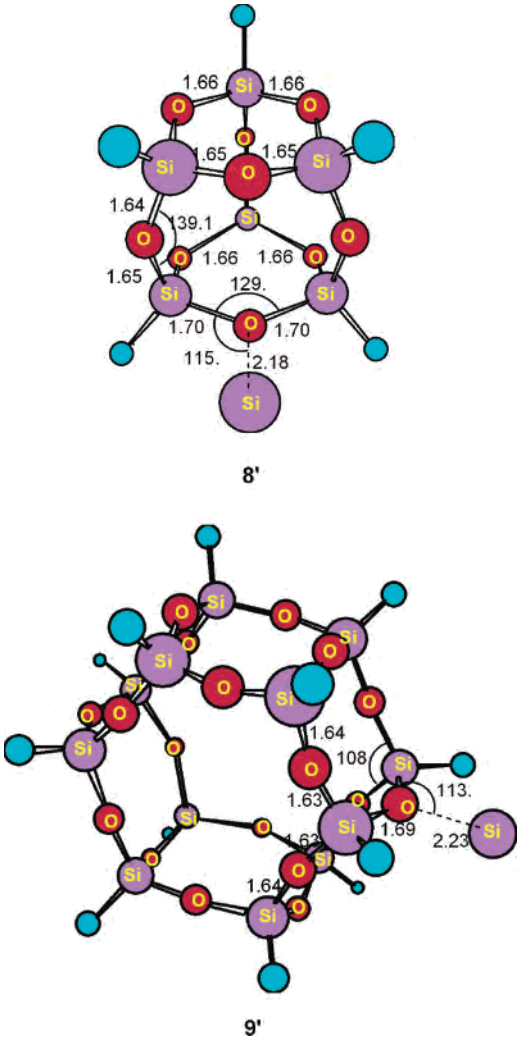

Figure 5. The **8′** and **9′** adducts resulting from the reaction of atomic silicon with molecules shown in Figure 1.

Table 2. Binding Energy E with Respect to Atoms of the Molecules Shown in Figure 1 and of the Corresponding Adducts, and Reaction Enthalpy ΔE of the Adducts with Respect to Reactants[a]

reactants	E [eV]	product	E [eV]	ΔE [kcal/mol]
2 **1** + Si	−79.12	$\mathbf{1}_2'$	−79.64	−12.0
2 **2** + Si	−95.58	$\mathbf{2}_2^{(0)}$	−96.10	−12.0
2 **3** + Si	−178.02	$\mathbf{3}_2'$	−178.75	−16.8
4 + Si	−81.57	**4′**	−81.78	−4.8
5 + Si	−123.13	**5′**	−123.41	−6.5
5 + Si	−123.13	**5″**	−123.26	−3.0
6 + Si	−139.40	$\mathbf{6}^{(0)}$	−139.88	−11.1
7 + Si	−164.57	**7′**	−164.91	−7.8
7 + Si	−164.57	**7″**	−164.80	−5.3
7 + Si	−164.57	**7‴**	−164.78	−4.8
8 + Si	−133.28	**8′**	−133.65	−8.5
9 + Si	−266.55	**9′**	−266.84	−6.7

[a] For the silicon atom in electronic state ^{3}P, a ground-state energy of −0.84 eV has been assumed, as recommended by Baerends et al.[19]

$2p_\sigma$ (40%) bonding with SiH_3 fragment, while the $4a_1$ orbital is mainly the $2p_\sigma$ located at the oxygen atom (44%); the empty $5b_1$ orbital represents the σ^* antibonding orbital between Si and H in plane, not involving oxygen atom.

From Table 3, we see that the singly occupied $6b_2$ orbital of $\mathbf{1}_2'$ has mainly silicon $3p_y$ orbital character, with a small mixing with **1** $5b_1$ and $6b_1$ (1) orbitals; analogously, the

Table 3. One-Electron Energies and Percentage Composition (Based on Mulliken Population Analysis per MO) of the Adduct Selected α Orbitals Involving Si Atom in Terms of Si and **N** Fragments[a]

	orbital	ϵ (eV)	Si	**N**
$\mathbf{1}_2'$	$6b_1\uparrow$	−3.77	92 $3p_x$	5 $5b_1$ + 2 $6b_1$ (2)
	$6b_2\uparrow$	−3.77	92 $3p_y$	5 $5b_1$ + 2 $6b_1$ (1)
	$9a_l\,\sigma$	−7.59	24 3s	37 $4a_1$ + 5 $3a_1$ (1), 37 $4a_1$ + 5 $3a_1$ (2)
	$8a_l\,\sigma$	−8.21	2 $3p_z$	44 $4a_1$ + 5 $3a_1$ (1), 44 $4a_1$ + 5 $3a_1$ (2)
	$7a_l\,\sigma$	−8.94	32 3s	26 $3a_1$ + 9 $4a_1$ (1), 26 $3a_1$ + 9 $4a_1$ (2)
	$6a_l\,\sigma$	−10.81	6 $3p_z$	43 $3a_1$ + 3 $4a_1$ (1), 43 $3a_1$ + 3 $4a_1$ (2)
$\mathbf{2}_2^{(0)}$	$14b\uparrow$	−3.36	98 $3p_y$ + 1 $3p_x$	1 11a (1) + (2)
	$15a\uparrow$	−3.54	98 $3p_z$	
	$7b\,\sigma$	−10.56	2 $3p_x$	31 6a + 43 7a + 13 8a + 7 9a + 3 10a + 1 12a
$\mathbf{3}_2'$	$15b_1\uparrow$	−5.07	92 $3p_x$	3 $9b_1$ + 1 $10b_1$ (2)
	$15b_2\uparrow$	−5.07	92 $3p_y$	3 $9b_2$ + 1 $10b_2$ (1)
	$12a_l\,\sigma$	−10.70	7 $3p_z$	28 $6a_1$ + 10 $8a_1$ + 8 $9a_1$ (1), 28 $6a_1$ + 10 $8a_1$ + 8 $9a_1$ (2)
4′	$8b_2\uparrow$	−3.70	91 $3p_y$	5 $8b_2$ + 1 $9b_2$
	$5b_1\uparrow$	−3.72	97 $3p_x$	1 $5b_1$ + 1 $4b_1$
	$8a_l\,\sigma$	−8.68	5 $3p_z$ + 49 3s	7 $6a_1$ + 38 $7a_1$ + 2 $8a_1$
5′	$14a_l\uparrow$	−3.44	94 $3p_z$	3 $13a_1$ + 1 $14a_1$
	$7b_2\uparrow$	−3.53	98 $3p_y$	2 $7b_2$
	$9b_1\,\sigma$	−9.75	3 $3p_x$	13 $8b_1$ + 78 $9b_1$ + 5 $11b_1$
5″	$12b_1\uparrow$	−3.52	92 $3p_x$	3 $12b_1$ + 1 $13b_1$
	$7b_2\uparrow$	−3.73	97 $3p_y$	2 $7b_2$
	$12a_1\,\sigma$	−8.71	3 $3p_z$ + 37 3s	22 $9a_1$ + 5 $10a_1$ + 25 $11a_1$ + 6 $12a_1$
$\mathbf{6}^{(0)}$	$8b_2\uparrow$	−3.15	99 $3p_y$	1 $8b_2$
	$16a_l\uparrow$	−3.33	98 $3p_z$	1 $15a_1$
	$11b_1\,\sigma$	−9.60	4 $3p_x$	8 $10b_1$ + 54 $11b_1$ + 3 $12b_1$ + 27 $13b_1$
7′	$18a_l\uparrow$	−3.48	92 $3p_z$	4 $17a_1$
	$9b_2\uparrow$	−3.57	97 $3p_y$	2 $9b_2$
	$12b_1\,\sigma$	−9.73	2 $3p_x$	9 $11b_1$ + 82 $12b_1$ + 5 $15b_1$
7″	$33a'\uparrow$	−3.89	92 $3p_y$ + 4 $3p_x$	1 32a′
	$16a''\uparrow$	−3.45	98 $3p_z$	1 15a″
	$28a'\,\sigma$	−8.58	1 $3p_x$ + 16 3s	48 26a′ + 3 27a′ + 7 28a′ + 21 29a′
7‴	$16b_1\uparrow$	−3.35	96 $3p_x$	1 $18b_1$
	$9b_2\uparrow$	−3.47	98 $3p_y$	1 $8b_2$
	$15a_1\,\sigma$	−8.57	3 $3p_z$ + 39 3s	29 $13a_1$ + 10 $14a_1$ + 19 $15a_1$

[a] The nature of contributions is also reported: (1) denotes **N** (**N** = 1, 3) lying in the *xz* plane, (2) denotes **N** (**N** = 1, 3) lying in the *yz* plane.

singly occupied $6b_1$ orbital is mainly a silicon $3p_x$ orbital mixing slightly with **1** $5b_1$ and $6b_1$ (2) orbitals. They have the same energy and both represent π_{ip} (in plane) orbital interactions between Si and **1** (1) and Si and **1** (2), respectively. The spatial extension of the silicon orbitals allows an appreciable overlap despite the large distance between Si and **1**. The occupied $6a_1$, $7a_1$, $8a_1$, and $9a_1$ orbitals have considerable **1** (1) and **1** (2) $4a_1$ and $3a_1$ character, with Si $3p_z$ and 3s contribution. They represent the σ bonding interactions between Si and a pair of **1**.

Inspection of Table 3 reveals that a similar Si−N molecular orbital pattern can be found for all the adducts, i.e., two singly occupied orbitals, mainly silicon $3p_\pi$ slightly mixing with a suitable empty **N** orbital, and fully occupied, low-lying in energy, orbitals, which are mainly occupied **N** orbitals slightly mixing with empty silicon $3p_\sigma$ orbital and/or silicon 3s orbital.

Table 4 shows the Mulliken gross population of α orbitals of **N** and Si fragments in the corresponding adducts. For the prototype adduct $\mathbf{1}_2'$, the π_{ip} orbital interaction in $6b_1$ causes

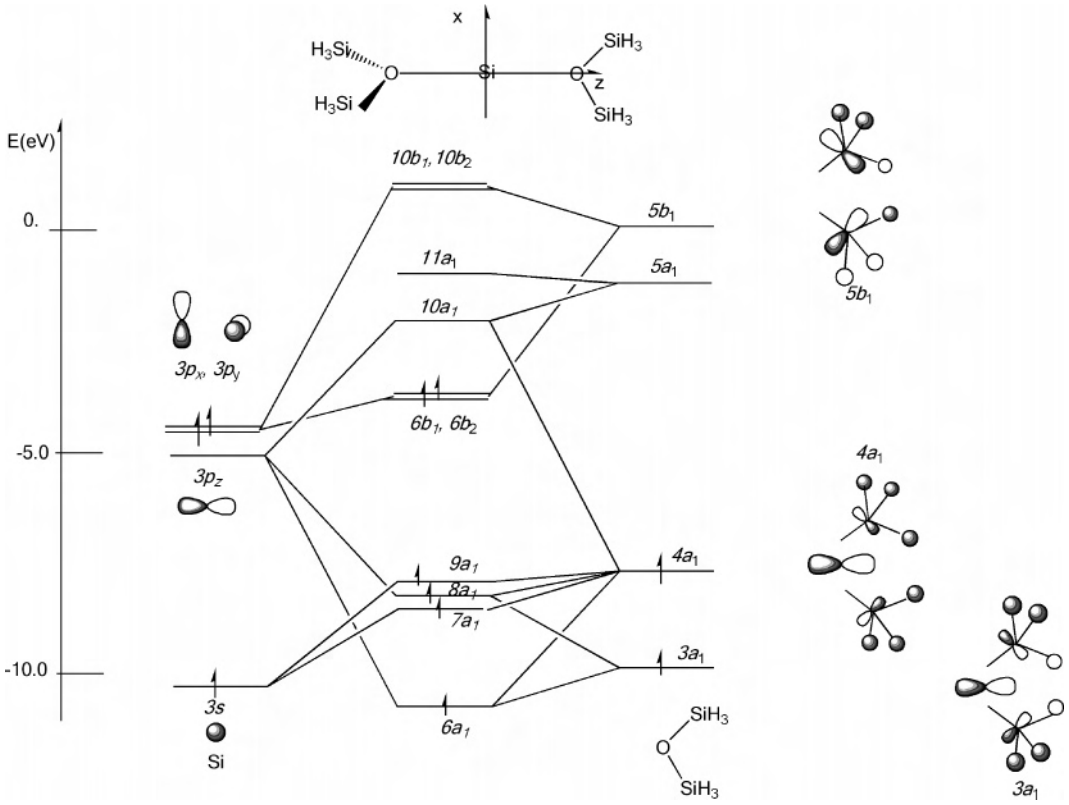

Figure 6. The orbital interaction diagram between Si atom and a pair of **1**. Only α spin−orbitals are shown.

Table 4. Mulliken Gross Population of SCF α Orbitals of **N** (**N** = 1−7) and Si Fragments in the Corresponding Adducts

Γ		$\mathbf{1}_2'$	$\mathbf{2}_2^{(0)}$	$\mathbf{3}_2'$	**4′**	**5′**	**5″**	$\mathbf{6}^{(0)}$	**7′**	**7″**[a]	**7‴**
σ	Si	3s 1.01	1.01	1.03	1.01	1.01	1.01	1.01	1.01	1.01	1.01
		$3p_\sigma$ 0.09	0.08	0.10	0.08	0.07	0.08	0.07	0.06	0.09	0.06
	N	$3a_1$ (1) 0.99	9a 0.98	$8a_1$ (1) 0.97	$7a_1$ 0.93	$9b_1$ 0.98	$10a_1$ 0.99	$11b_1$ 0.97	$12b_1$ 0.98	27a′ 0.99	$15a_1$ 0.95
		$4a_1$ (1) 0.97	10a 0.98	$9a_1$ (1) 0.97	$8a_1$ 1.00	$11b_1$ 0.97	$11a_1$ 0.94	$13b_1$ 0.97	$15b_1$ 0.97	29a′ 0.96	
		$3a_1$ (2) 0.99	12a 0.98	$8a_1$ (2) 0.97							
		$4a_1$ (2) 0.97		$9a_1$ (2) 0.97							
π_{ip}	Si	$3p_x$ 0.94	$3p_z$ 0.99	$3p_x$ 0.94	$3p_y$ 0.94	$3p_z$ 0.96	$3p_x$ 0.95	$3p_z$ 0.99	$3p_z$ 0.94	$3p_y$ 0.93	$3p_x$ 0.97
		$3p_y$ 0.94	$3p_y$ 0.99	$3p_y$ 0.94							
	N	$5b_1$ (2) 0.05		$9b_1$ (2) 0.03	$8b_2$ 0.05	$13a_1$ 0.03	$12b_1$ 0.03	$15a_1$ 0.01	$17a_1$ 0.04	32a′ 0.01	$18b_1$ 0.01
		$6b_1$ (2) 0.02		$10b_1$ (2) 0.01	$9b_2$ 0.01	$14a_1$ 0.01	$13b_1$ 0.01				
		$5b_1$ (1) 0.05		$9b_2$ (1) 0.03							
		$6b_1$ (1) 0.02		$10b_2$ (1) 0.01							
π	Si				$3p_x$ 0.99	$3p_y$ 0.99	$3p_y$ 0.99	$3p_y$ 1.00	$3p_y$ 0.98	$3p_z$ 1.00	$3p_y$ 1.00
	N				$5b_1$ 0.01	$7b_2$ 0.02	$7b_2$ 0.02	$8b_2$ 0.00	$9b_2$ 0.02	16a″ 0.00	$9b_2$ 0.00
spin dens		1.93	2.02	1.92	1.95	1.98	1.97	2.02	1.95	1.99	1.99
gross char		−0.09	−0.16	−0.20	−0.12	−0.11	−0.14	−0.14	−0.05	−0.09	−0.10

[a] The σ and π_{ip} populations of α orbitals have to be considered together (adducts in C_s symmetry).

a slight decrease in the Si $3p_x$ spin α Mulliken population which reduces from l*e* to 0.94*e*, and a corresponding increase of the **1** $5b_1$ (1) α population (0.05*e*) and $6b_1$ (1) α population (0.02*e*). The Si $3p_x$ β spin population, not shown in Table 4, is small (0.01*e*). The π_{ip} orbital interaction in $6b_2$ decreases analogously the Si $3p_y$ spin α Mulliken population to 0.94*e*, and increases the **1** $5b_1$ (2) α population (0.05*e*) and the **1** $6b_1$ (2) α population (0.02*e*). The orbital combinations in the occupied $8a_1$ and $6a_1$ shown in Table 3 MO (Si $3p_\sigma/3a_1$, $4a_1$ of **1**) populate the Si $3p_1$ by 0.09*e* (α spin) and 0.07*e* (β spin) coming from $3a_1$ (0.99*e* α, 0.99*e* β) and $4a_1$ (0.97*e* α, 0.97*e* β) of both **1** fragments, (1) and (2).

As a general trend for all the adduct series, in σ symmetry, a small electron donation takes place from the **N** occupied orbitals to silicon $3p_\sigma$. It is worth noting that there are only minor differences in the σ charge transfers along the adduct series; i.e., the Si $3p_\sigma$ population is in the narrow range from 0.06*e* to 0.10*e*. In π_{ip} and π out of plane symmetries, a small to a very small electron back-donation occurs from silicon $3p_\pi$ orbitals to empty **N** orbitals. The π_{ip} back-donation is clearly more involved in the bonding, as demonstrated by the larger charge transfer from Si $3p_{\pi_{ip}}$, whose α spin population ranges from 0.93 to 0.99*e* in the series. In π out of plane symmetry, the Si−N interaction is much less effective, since the Si $3p_\pi$ α spin population remains invariably 0.99*e* and 0.01*e* are found in the β spin counterpart of the Si $3p_\pi$ orbital. The calculated spin density at silicon, which is also reported in Table 4, is always very close to 2 electrons, in agreement with the previously described electronic structure and Mulliken population analysis of the

Table 5. Decomposition of the Bonding Energy for the Formation of the Adducts in Terms of Si and the Corresponding Model Molecule **N** Fragments[a]

	$\Delta E°$	ΔE_σ	$\Delta E_{\pi_{ip}}$	ΔE_π	ΔE_{oi}	ΔE_{total}	ΔE_{prep}	ΔE
1′	1.32	−1.17	−0.90	−0.73	−2.81	−1.49	1.01	−0.48
$\mathbf{1}_2'$	1.19	−1.04	−0.83, −0.83		−2.70	−1.50	0.98	−0.52
$\mathbf{3}_2'$	1.10	−1.10	−0.90, −0.90		−2.91	−1.81	1.08	−0.73
4′	1.30	−0.94	−1.02	−0.66	−2.62	−1.32	1.11	−0.21
5′	0.89	−0.50	−1.07	−0.59	−2.17	−1.29	1.00	−0.28
5″	1.38	−0.84	−1.10	−0.63	−2.58	−1.20	1.07	−0.13
$\mathbf{6}^{(0)}$	0.46	−0.51	−0.77	−0.57	−1.88	−1.42	0.94	−0.48
7′	0.77	−0.41	−1.04	−0.57	−2.04	−1.27	0.93	−0.34
7‴	0.82	−0.63	−0.75	−0.59	−1.97	−1.15	0.94	−0.21
			$\Delta E_\sigma + \Delta E_{\pi_{ip}}$	ΔE_π	ΔE_{oi}	ΔE_{total}	ΔE_{prep}	ΔE
7″	0.80		−1.41	−0.58	−1.99	−1.19	0.96	−0.23
			$\Delta E_\sigma + \Delta E_\pi$	$\Delta E_{\pi_{ip}}$	ΔE_{oi}	ΔE_{total}	ΔE_{prep}	ΔE
$\mathbf{2}_2^{(0)}$	0.49		−1.14	−0.81	−1.95	−1.46	0.94	−0.52

[a] $\Delta E°$ is the steric repulsion, the $\Delta E(\Gamma)$ values are the contributions due to orbital interaction in σ (ΔE_σ) and π in plane ($\Delta E_{\pi_{ip}}$) and out of plane (ΔE_π) symmetries, ΔE_{oi} is the total orbital interaction contribution, ΔE_{total} is the sum of $\Delta E°$ and ΔE_{oi}. Preparation energies (ΔE_{prep}) of the fragments and bonding energies (ΔE) of the adducts are also given.

adducts. The calculated total Mulliken gross charge on silicon (see Table 4) is slightly negative in the adduct series, also in agreement with the calculated σ electron donation from oxo-oxygen to silicon.

Bonding Energy Analysis. The charge rearrangements are a qualitative indication for the bonding interactions, but not a quantitative measure of the corresponding energies. Those are explicitly calculated by the energy decomposition scheme discussed in section 2 and displayed in Table 5. In order to have clear and meaningful energy contributions in the individual σ and π symmetries, we use valence state of Si $3s^2 3p_\sigma{}^0 3p_{\pi_{ip}}{}^1 3p_\pi{}^1$ as found in the adduct situation. This change of configuration has the advantage that the empty $3p_\sigma$ can act as acceptor orbital for electrons from the occupied oxo-oxygen orbitals. For **N**, we use the geometry of the fragment as it occurs in the adduct.

As shown in the first column of Table 5, the steric interaction energy $\Delta E°$ is repulsive, mainly due to the positive, destabilizing Pauli repulsion term, which reflects the number of closed shell electrons. Looking first at $\mathbf{1}_2'$ and $\mathbf{3}_2'$ adducts, we note that the $\Delta E°$ term becomes less positive, behaving approximately as a function of the Si−O distance. In **5′**, **5″** and **7′**, **7″**, and **7‴** series, the steric interaction term becomes more positive down the series reflecting the increasing strain. The largest $\Delta E°$ is calculated for **8′**, representing a rigid siloxanic network, while the smallest $\Delta E°$ values are calculated for $\mathbf{6}^{(0)}$ and $\mathbf{2}_2^{(0)}$, because of the decreased strain for silicon which interacts with a terminal oxo-oxygen. As far as the orbital interaction energies are concerned, ΔE_{oi}, they are stabilizing in all investigated adducts, and they are invariably larger than the steric terms, $\Delta E°$, thus determining the final stability of the adducts. The decomposition in energy contributions belonging to different symmetries (σ, π, and π_{ip}) does not distinguish charge transfer and polarization. However, since we are considering neutral interacting fragments (Si and N), it is expected that polarization is relatively small. Moreover, the "pure" σ contribution can be calculated only for adducts characterized by a C_{2v} symmetry, while for adducts in C_s (**7″** and **8′**) and C_2 ($\mathbf{2}_2^{(0)}$) symmetries the σ contribution cannot be separated from π_{ip}, or π out of plane, contribution. Considering the data collected in Table 5 for adduct $\mathbf{1}_2'$, we note that the σ donation from oxo-oxygen into Si $3p_\sigma$ orbital of 0.09*e* (α) and 0.07*e* (β) has an energy contribution of −1.04 eV. The π_{ip} α spin back-donation out of Si $3p_x$ and $3p_y$ into σ^* orbitals of the adjacent Si−H bonds in the same plane of 0.06 α electrons gives each an equal contribution to the total energy which is −0.83 eV.

As a general result for all the adduct series, from the data reported in Table 5, the ΔE_σ term that accounts for σ donation from **N** into $3p_\sigma$ silicon orbital varies in the range between −1.10 and −0.41 eV. The smallest ΔE_σ values are calculated for **5′**, $\mathbf{6}^{(0)}$, **7′**, and **7‴** and are in agreement with the somewhat smaller charge transfer (see Table 4). As for the energy terms which account for the π interaction, the ΔE_π term is always smaller than the $\Delta E_{\pi_{ip}}$ one, reflecting mainly a polarization effect instead of charge transfer from silicon $3p_\pi$ out of the plane. While the value for ΔE_π has contributions along the series between −0.57 and −0.78 eV, the $\Delta E_{\pi_{ip}}$ varies in the range between −1.10 and −0.75 eV, in line with the variation of the charge transfers from silicon $3p_{\pi_{ip}}$ into σ^* orbitals of the **N** fragment observed in this symmetry. As a result of these contributions, the total bonding energy term, ΔE_{total}, is stabilizing for all the adducts, but the preparation energy of the fragments has to be taken into account in order to get the reaction enthalpy ΔE for the formation of the adducts. It is interesting to note, however, that despite the repulsive contributions of $\Delta E°$ and ΔE_{prep} the bond energy ΔE is negative (bonding) for all the adducts.

The preparation energy, ΔE_{prep}, is largely dominated by the energy necessary to excite the silicon atom from the ground electronic configuration to singly populate the $3p_\pi$ orbitals as we calculate in the converged adducts (i.e., 0.92 eV). The remaining value represents the geometry change of **N** bonding to Si in the adduct. Since the major variation is calculated to be the Si−O−Si angle of the disiloxo center involved in the bond, we expect that the larger ΔE_{prep} is, the closer the oxygen bond configuration is to a trivalent oxygen coordinating one Si atom and two $Si^{(4)}$, and the larger the ΔE_σ is, due to electron shifts from oxygen to Si, with Si behaving as a Lewis acid. The recognition that silicon can behave as a Lewis acid in these adducts is in agreement with

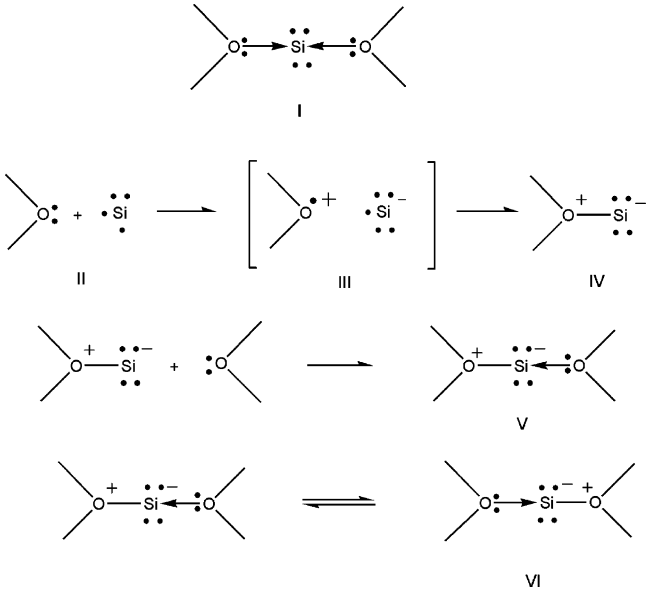

Figure 7. Structural formulas for oxo-oxygen−silicon bonds for silicon in singlet state (**I**) or in triplet state.

ab initio calculations by Deák et al.[20] which demonstrates that a 3-fold coordinated oxygen can act as a donor to silicon. Indeed, from Table 5, we can see that to the largest ΔE_{prep} terms, calculated for $\mathbf{3}_2'$, **4′**, and **5″** adducts, correspond the largest ΔE_σ contributions to the bonding energies. The $\mathbf{6}^{(0)}$ and $\mathbf{2}_2{}^{(0)}$ adducts are quite different from the other adducts in that the trivalent oxygen coordinates the silicon atom, a hydrogen, and a $Si^{(4)}$. The geometry rearrangement of **6** bonding to Si, for instance, is very small (ΔE_{prep} 0.02 eV), and the steric constraints are also small (ΔE^0 0.46 eV), but it is interesting to note that only for $\mathbf{6}^{(0)}$ (and probably also for $\mathbf{2}_2{}^{(0)}$) the energy contribution due to σ donation from oxygen to Si (ΔE_σ) is larger, in absolute value, than $\Delta E_{\text{prep}} + \Delta E°$; i.e., the σ donation alone is able to stabilize this adduct.

The above detailed analysis of the different contributions to ΔE_{oi} points out that in the adduct series (i) the σ interactions between the silicon atom and the model molecules **N**, due to electron donation from oxo-oxygen to silicon, account for 20−39% of the bond strength; (ii) π back-donation from silicon $3p_\pi$ to empty σ^* antibonding **N** orbitals gives an important contribution to silicon−**N** interaction.

A Lewis Description of the Oxo-Oxygen−Silicon Bond. Using an arrow to denote a dative bond, formula **0** can indeed be written as **I** in Figure 7. This formula attributes to $Si^{(0)}$ in triplet configuration the character of bifunctional Lewis acid. This is possible only if one electron shifts from oxygen to silicon (**II** → **III** in Figure 7) and a covalently bonded species **IV** is eventually formed between the resulting species. Adduct **IV** contains a residual Lewis acid function and is thus able to bind to another oxo-oxygen accepting a lone electron pair, thus forming species **V**. The second acid−base bond is however expected to be appreciably weaker than the first one because the net charge on the acidic function (silicon) is negative (though slightly), a quite strange situation in acid−base phenomenology. If the distance of the second oxygen atom is not subjected to steric constraints, the di-oxo-oxygen−silicon complex may attain a symmetric configuration, in which case the two equivalent configurations **V** and **VI** may be stabilized by resonance.

In order to test the argument that Si behaves as a Lewis acid according to the above description, geometry optimization calculation has been performed also on the **1′** adduct, i.e., the corresponding species **IV** in Figure 7. The triplet state of the adduct is still the configuration of minimum energy. The main differences in the geometrical parameters with respect to $\mathbf{1}_2'$ are the Si−O distance, which is shorter (2.11 Å vs 2.39 Å), and the Si−O−Si angle of the siloxo center involved in the interaction with Si, which is smaller (137° vs 140°). The adduct **1′** is found to be thermodynamically more stable than reactants by −0.48 eV, to be compared to −0.52 eV for $\mathbf{1}_2'$, as shown in Table 5. The electronic structure of **1′** is very similar to that of $\mathbf{1}_2'$, i.e., two singly occupied orbitals, $3b_2$, mainly silicon $3p_\pi$ slightly mixing with occupied $2b_2$ of **1**, and $4b_1$, mainly silicon $3p_{\pi_{ip}}$, slightly mixing with $5b_1$ of **1**. Unlike $\mathbf{1}_2'$ one of the silicon $3p_\pi$ orbitals is completely available for π interaction out of plane (singly occupied $3b_2$ orbital). Two fully occupied, low-lying in energy, orbitals, $3a_1$ and $5a_1$, describe σ interaction between empty silicon sp_σ orbitals and occupied $3a_1$ and $4a_1$ orbitals of **1**. From the Mulliken population analysis of α orbitals of **1** and Si fragments in adduct **1′**, we find that Si $3p_\sigma$ orbital populates by 0.09*e* (α spin) because of donation from $3a_1$ (0.97*e* α) and $4a_1$ (0.94*e* α) of **1**, and Si $3p_{\pi_{ip}}$ population decreases to 0.90*e* (α spin) going to $4b_1$, (0.01*e* α), $5b_1$ (0.06*e* α), and $6b_1$ (0.03*e* α) empty orbitals of **1**. For Si $3p_\pi$ population, it changes only very little (0.99*e* α), with 0.01*e* going to β spin counterpart of Si $3p_\pi$ orbital. As a result, the spin density on Si is 1.92, while the calculated total Mulliken gross charge on silicon is slightly negative (−0.10). From the bonding energy analysis in Table 5, we note that the σ donation from oxo-oxygen into Si $3p_\sigma$ orbital has an energy contribution of −1.17 eV, which is slightly larger than that of $\mathbf{1}_2'$ (−1.04 eV), and this is in agreement with the smaller Si−O distance. The π_{ip} α spin back-donation out of Si $3p_\pi$ into σ^* orbitals of the adjacent Si−H bonds in the same plane gives a contribution of −0.90 eV to the total energy, again slightly larger than that of $\mathbf{1}_2'$ adduct (−0.83 eV). Finally, the π interaction out of plane contributes to the total energy by −0.73 eV, which is mainly due to polarization effects instead of charge donation. We conclude that adduct **1′**, corresponding to species **IV** of Figure 7, can be described as a covalently bonded species resulting from electron shifting from oxygen to silicon, and that adduct **1′** (species **IV** in Figure 7) contains a residual Lewis acid function able to bind to another oxo-oxygen accepting electrons and thus forming adduct $\mathbf{1}_2'$ (species **V**−**VI** in Figure 7). Actually, the two equivalent configurations **V** and **VI** in Figure 7 show some stabilization by resonance, though

(19) Baerends, E. J.; Branchadell, V.; Sodupe, M. *Chem. Phys. Lett.* **1997**, *265*, 481.
(20) (a) Deák, P.; Snyder, L. C.; Corbett, J. W. *Phys. Rev. Lett.* **1991**, *66*, 747. (b) Deák, P.; Snyder, L. C.; Corbett, J. W. *Phys. Rev. B* **1992**, *45*, 11612.

very small, which can be calculated by the energy difference between −0.48 eV of **1′** and −0.52 eV of $\mathbf{1}_2'$ adducts.

4. Conclusions

The existence of atomic silicon in siloxanic networks has been theoretically investigated through density functional calculations. Modeling with model molecules the candidate sites to host atomic silicon, we found that all molecules not imposing strong steric constraints to the formation of center **0** are able to bind silicon. The triplet state of the adducts is always more stable than the singlet one, and it invariably contains a Si atom with a slightly negative charge which retains most of its atomic characteristics and carries two unpaired electrons on its $3p_\pi$ orbitals. When the steric constraint becomes too strong, atomic silicon binds to one oxygen atom only. In conclusion, our study supports the view that atomic silicon injected in bulk SiO_2 cannot be trapped therein in localized states; stationary localized states are possible only at the surface where the reticulation degree of the oxide is partially lost because of hydroxyl terminations. Detailed analysis of the nature of oxo-oxygen−silicon bond at the SiO_2 surface reveals that the silicon is kept at the surface in atomic-like configuration by (i) σ charge donation from oxo-oxygen atoms into the empty silicon $3p_\sigma$ (or sp_σ) orbital; (ii) π charge back-donation from singly occupied silicon $3p_\pi$ orbitals into the empty σ^* model molecule orbitals. These results attribute to atomic silicon the character of bifunctional Lewis acid which, surprisingly, carries on the acidic function (silicon) a negative (though slight) net charge.

IC048927D